

Fundus autofluorescence imaging in dry AMD: 2014 Jules Gonin lecture of the Retina Research Foundation

Frank G. Holz · Julia S. Steinberg · Arno Göbel ·
Monika Fleckenstein · Steffen Schmitz-Valckenberg

Received: 30 October 2014 / Accepted: 3 November 2014 / Published online: 19 November 2014
© Springer-Verlag Berlin Heidelberg 2014

Abstract Fundus autofluorescence (FAF) imaging allows for topographic mapping of intrinsic fluorophores in the retinal pigment epithelial cell monolayer, as well as mapping of other fluorophores that may occur with disease in the outer retina and the sub-neurosensory space. FAF imaging provides information not obtainable with other imaging modalities. Near-infrared fundus autofluorescence images can also be obtained *in vivo*, and may be largely melanin-derived. FAF imaging has been shown to be useful in a wide spectrum of macular and retinal diseases. The scope of applications now includes identification of diseased RPE in macular/retinal diseases, elucidating pathophysiological mechanisms, identification of early disease stages, refined phenotyping, identification of prognostic markers for disease progression, monitoring disease progression in the context of both natural history and interventional therapeutic studies, and objective assessment of luteal pigment distribution and density as well as RPE melanin distribution. Here, we review the use of FAF imaging in various phenotypic manifestations of dry AMD.

Keywords Fundus autofluorescence · Age-related macular degeneration · Drusen · Reticular drusen · Geographic atrophy · Foveal sparing · Scanning laser ophthalmoscopy · Image analysis

Introduction

Fundus autofluorescence (FAF) imaging allows for topographic mapping of lipofuscin (LF) distribution in the retinal

pigment epithelial (RPE) cell monolayer, as well as mapping of other fluorophores that may occur with disease in the outer retina and the sub-neurosensory space [1, 2]. FAF imaging provides additional information not obtainable with other imaging modalities such as fundus photography, fluorescein angiography, or OCT. Excessive accumulation of LF granules in the lysosomal compartment of RPE cells represents a common downstream pathogenetic pathway in various hereditary and complex retinal diseases [3].

Near-infrared fundus autofluorescence (NIA) images can also be obtained *in vivo* using the indocyanine green angiography mode. It has been suggested that the NIA signal is largely melanin-derived [4].

The recording of FAF images is a non-invasive procedure. The intensity of naturally occurring fluorescence of the ocular fundus is about two orders of magnitude lower than the background of a fluorescein angiogram at the most intense part of the dye transit. Both scanning laser ophthalmoscopy and fundus camera photography have been used in the clinical setting for the acquisition of fundus autofluorescence images [5–7]. Confocal scanning laser ophthalmoscopy (cSLO) optimally addresses the limitations of the low intensity of the autofluorescence signal and the interference of the crystalline lens.

FAF imaging has been shown to be useful in a wide spectrum of macular and retinal diseases [8]. The scope of applications now includes identification of diseased RPE in macular/retinal disorders, elucidating pathophysiological mechanisms, identification of early disease stages, refined phenotyping, identification of prognostic markers for disease progression, monitoring disease progression in the context of both natural history and interventional therapeutic studies, and objective assessment of luteal pigment distribution and density as well as RPE melanin distribution. Herein we review the use of FAF imaging in various manifestations of dry AMD.

F. G. Holz (✉) · J. S. Steinberg · A. Göbel · M. Fleckenstein ·
S. Schmitz-Valckenberg
Department of Ophthalmology, University of Bonn, Ernst-Abbe-Str.
2, 53127 Bonn, Germany
e-mail: frank.holz@ukb.uni-bonn.de

Early AMD

FAF findings in early and intermediate AMD may indicate more widespread abnormalities and diseased retinal areas than revealed by funduscopy or color fundus photography (CFP) alone (Fig. 1). Early manifestations of AMD include areas of focal hypo- and hyperpigmentation at the level of the RPE, drusen with extracellular material accumulating in the inner aspects of Bruch's membrane, as well as reticular drusen with abnormalities assumed to be located at the RPE–photoreceptor interface [9–11].

Areas of focal hyperpigmentation are usually associated with increased FAF signal intensity (Fig. 1d), which is thought to derive from melanolipofuscin, whereas depigmentation is characterized by a reduced FAF signal due to loss of RPE. Hence, FAF imaging compared to CFP is better able to identify even small non-central areas of GA (Fig. 2), the existence of which defines late AMD, according to a recently introduced new AMD clinical classification system [10].

The FAF signal from individual drusen may be slightly increased, unchanged, or decreased compared to normal background FAF [12]. The composition of drusen, drusen size, and alterations in the overlying RPE may be responsible for such variability in corresponding FAF signal intensity. In general, larger drusen are more frequently associated with extensive FAF changes than smaller drusen [13] (Figs. 1a/b). Crystalline drusen typically show a corresponding area of lower FAF signal (Fig. 1c). In contrast, large soft confluent drusen or drusenoid RPE detachments are usually characterized by increased signal intensity [13] (Fig. 3). Depending on lesion size and resolution of imaging methods, it may be challenging to assign a specific quality of change in FAF (i.e., increased or decreased intensity) to each drusenoid lesion. Indeed, studies using a fundus camera for FAF imaging noted a central area of decreased FAF surrounded by an annulus of increased FAF that was correlated with soft drusen between 60 and 175 μm in size [14].

An international consensus group distinguished eight distinctive FAF patterns in early AMD [12]: normal, minimal change, focal increased, patchy, linear, lacelike, reticular, and speckled (Fig. 4). This phenotypic classification may help to identify prognostic determinants in longitudinal studies and to explore phenotype–genotype as well as structure–function correlations in future investigations.

Landa et al. investigated SD-OCT–cSLO FAF correlations in patients with bilateral early AMD in areas of drusen primarily detected by SD-OCT [15], noting that disruptions in the outer retina (i.e., the IS/OS junctional layer) were closely related to local FAF changes. However, they did not report on specific FAF changes, i.e., increased or decreased signals. This is consistent with other reports on sensitivity reduction in areas with altered FAF compared to areas with normal FAF [16].

The FAF signal may also change following drusen regression. Toy and colleagues noted a prominent decrease or increase in FAF signal at areas of drusen regression in 64 % and 14 % of eyes, respectively. They were unable to detect significant changes in the photoreceptor layer using SD-OCT, however, reflecting the general lack of clarity regarding the short- and long-term consequences of drusen regression [17].

In a review article on different types of drusen in AMD, Mimoun and colleagues described—in addition to other well-defined soft, hard, calcified, and cuticular drusen—“pseudodrusen visible en lumière bleu” [pseudodrusen visible in blue light] [11]. The distinctive characteristic appearance of these subtle alterations was subsequently reported by others using different terms, including “reticular drusen” (RD) [18], “reticular pattern” [13], “reticular pseudodrusen” [19], “reticular macular disease” [20], and “subretinal drusenoid deposits” [21]. This lack of uniformity in nomenclature may be a result of parallel description using different retinal imaging modalities, the very small and subtle alterations that exist, and the yet unclear histopathological correlation. Irrespective of the location of RDR lesions within the retina or of the terminology, it is a consistent finding that the *in vivo* detection of these lesions not only requires good image quality, but that combined near-infrared (NIR) and FAF confocal scanning laser ophthalmoscopy (cSLO), as well as spectral-domain optical coherence tomography (SD-OCT) imaging, represent the modalities of choice for their *in vivo* identification [9, 21]. FAF imaging reveals a unique reticular pattern with multiple small rounded or elongated areas of decreased FAF surrounded by areas with brighter intensities (Fig. 5) [9].

Use of these imaging modalities in a large cohort of patients with geographic atrophy revealed that the prevalence of RD was much higher than expectations based on a previous smaller series with less adequate imaging methods. Concurrent RD was present in more than 60 % of eyes with outer retinal atrophy [22]. Several studies have indicated that RD may represent a high risk factor for the progression to late AMD [23, 19, 18, 24].

At this time, little is known about the natural history of RD, i.e., longitudinal changes over time. Using *en face* cSLO fundus autofluorescence imaging in patients with geographic atrophy secondary to AMD, we demonstrated that the area with RD involvement increased over a period of 18 months, and that progression in this area occurred at a rate at least four times that of the total area of atrophy [25].

Geographic atrophy

FAF imaging has proven particularly useful for various aspects in the context of geographic atrophy (GA) secondary to AMD. Due to the absence of RPE cells, and thus the loss of intrinsic LF fluorophores, atrophic areas in patients with GA

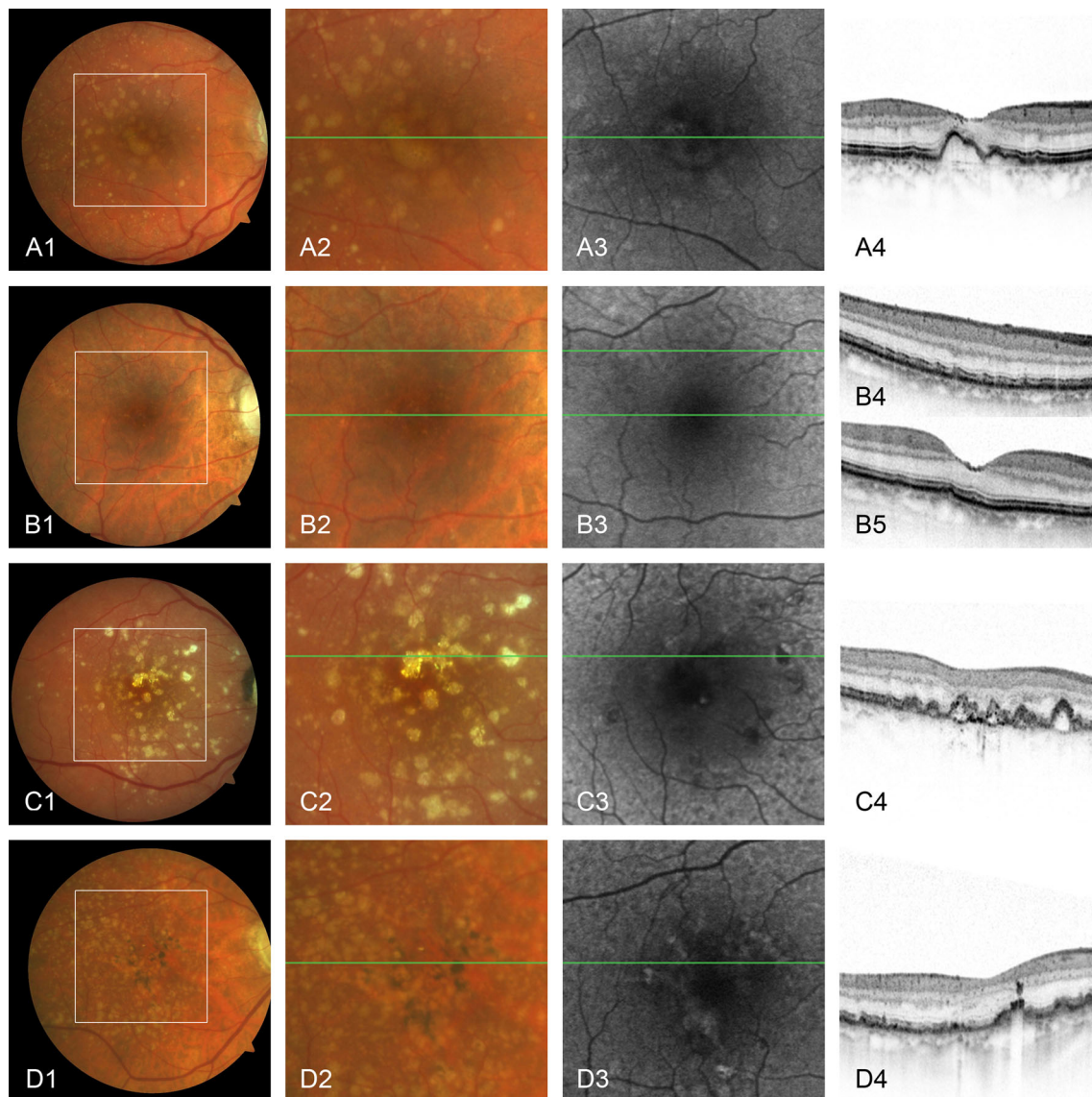


Fig. 1 Different manifestations of intermediate AMD (**a, c, d**) and normal changes associated with aging (**b**). Soft confluent drusen (**A1, A2**) reveal a slightly increased FAF signal (**A3**) and a characteristic dome-shaped elevation of outer retinal layers in SD-OCT (**A4**). Drupelets (small drusen) (**B1, B2**) represent normal changes with aging, and also cause elevation of the outer retinal layers (**B5**). In reticular pseudodrusen, which can be better identified in FAF than in CFP imaging (**B3**), SD-OCT

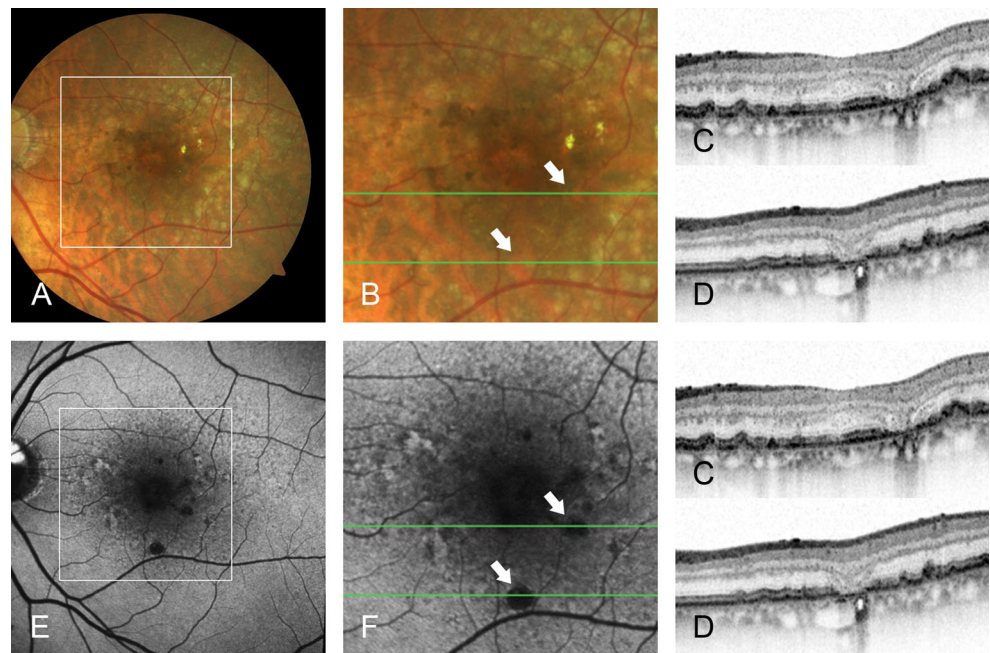
suggests alterations at the level of the photoreceptors (**B4**). Crystalline or calcified drusen (**C1, C2**) often correspond to a lower FAF signal (**C3**) and inhomogeneous inner reflectivity in SD-OCT (**C4**). Areas of focal hyperpigmentation (**D1, D2**) are mostly confined to increased FAF (**D3**) and focal hyperreflectivity at the level of the RPE or the more inner retinal layers in SD-OCT (**D4**)

exhibit a severely reduced signal (Fig. 6) [3, 2]. FAF imaging using an excitation wavelength of 488 nm and an emission bandwidth of 500–700 nm showed that areas of GA exhibited very low to extinguished FAF signals (dark), with a high contrast between the area of atrophy and perilesional retina (Fig. 7). Contrast levels rose even further with the commonly observed finding that the perilesional zone showed high FAF intensities. Perilesional FAF changes, in particular, appear to have pathogenetic relevance: areas of increased FAF, and hence lipofuscin accumulation outside GA, may be associated with varying degrees of retinal sensitivity loss, and precede

the development and enlargement of outer retinal atrophy (Fig. 7) [12, 26–28]. These findings correlate with experimental data suggesting that certain molecular compounds of LF such as N-retinylidene-N-retinylethanolamine (A2-E) may possess toxic properties upon reaching a critical level and may interfere with normal cell function [29, 30].

The high contrast to the perilesional non-atrophic retina allows for exact delineation and segmentation of atrophic areas using grey-value-based region-growing algorithms in semi-automated software. Further technological development recently led to the release of the “RegionFinder” software

Fig. 2 Left eye of a patient with areas of focal hyper- and hypopigmentation and soft confluent drusen. FAF (e) reveals more pronounced changes than CFP (a). In particular, small non-central areas of geographic atrophy are clearly visible, whereas on CFP (a), corresponding depigmented areas are less remarkable. SD-OCT through two of these lesions (white arrows) reveals choroidal hyperreflectivity and loss of the photoreceptor layer, both typical findings in geographic atrophy (c and d)



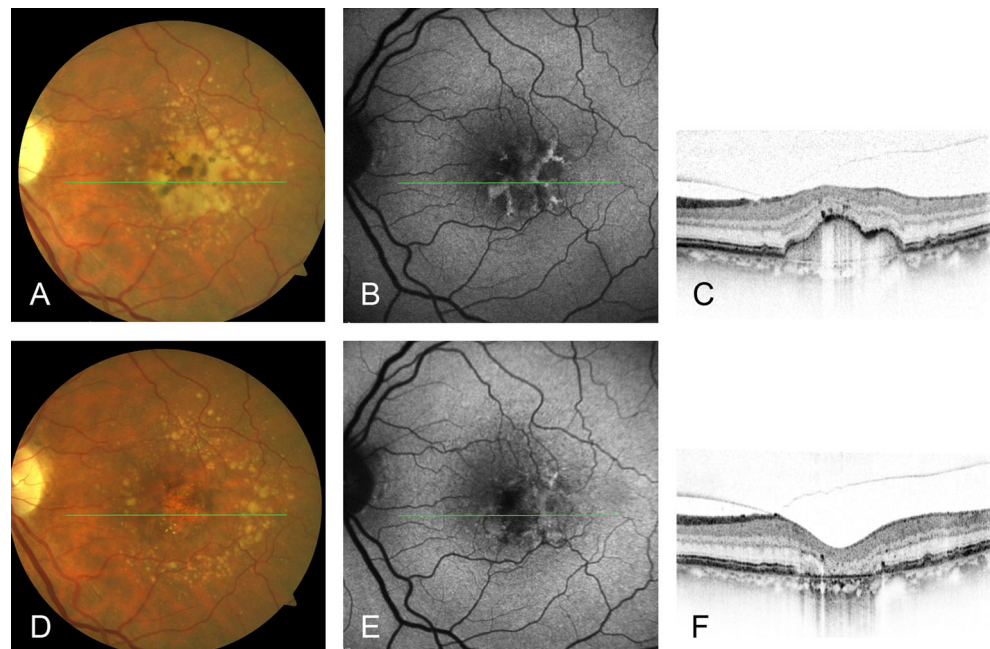
(Heidelberg Engineering, Heidelberg, Germany) (Fig. 8). This image processing tool allows for rapid, reproducible semi-automated detection and measurement of the size and progression of atrophic GA areas [31]. Its functions comprise direct export and alignment of recorded images, semi-automated identification of atrophic patches after selecting a seeding point and adjusting tolerance levels, shadow correction, semi-automated vessel detection, and creation of a report displaying the results of the analysis. Its application is suitable not only for analysis of progression rates in natural history studies or interventional trials designed to slow the disease

process, but also for routine use in clinical practice for documenting individual patient disease progression.

At times, quantification of GA based on FAF images alone may be challenging, particularly in the central retina. This is primarily due to low FAF intensity in the fovea due to absorption of short-wavelength light by luteal pigment. Utilizing corresponding blue reflectance (BR 488 nm) and near-infrared reflectance (IR 820 nm) images may help to improve foveal lesion boundary discrimination.

Various longitudinal natural history studies have independently reported high interindividual variation in atrophy

Fig. 3 Left eye of a patient with intermediate AMD with large, confluent soft drusen and areas of focal hyperpigmentation at baseline (upper row) and development of geographic atrophy after two years (lower row). At baseline, the FAF signal shows a lacelike pattern (b), whereas after two years, a markedly lower signal at the area of atrophy is evident (e). Drusen regression is most remarkable in CFP (a and d)



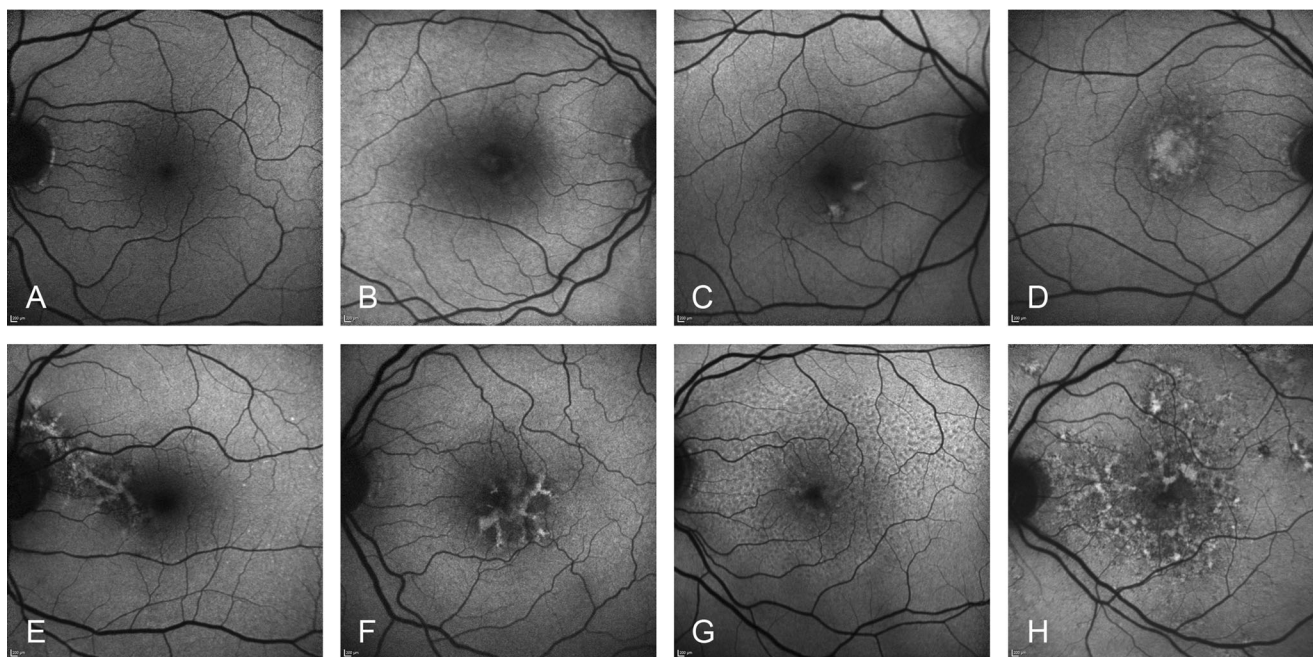


Fig. 4 Different FAF patterns in early and intermediate AMD: normal (a), minimal change (b), focal increased (c), patchy (d), linear (e), lacelike (f), reticular (g), and speckled (h). The Association for Research in Vision

and Ophthalmology (ARVO), as the copyright holder, has kindly granted copyright permission for the use of this figure, which was adapted from Bindewald and colleagues [12]

progression that cannot be explained by genetic or exogenous factors [32–34, 7, 35]. There is evidence that more specific individual characteristics may at least partially explain the high interindividual variability in the spread of atrophy. The FAM (Fundus Autofluorescence in Age-Related Macular Degeneration, www.clinicaltrials.gov, NCT00393692) study has identified different phenotypic patterns of abnormal FAF in the junctional zone of GA based on cSLO FAF imaging, describing a step-wise classification approach (Fig. 9) [12, 34, 36, 37]. Analysis of longitudinal FAF imaging data has shown the prognostic relevance of these patterns of GA enlargement over time [34].

Rates of atrophy progression were slowest in eyes without abnormal FAF in the perilesional zone (median 0.38 mm²/year), followed by eyes with focal increased FAF (median

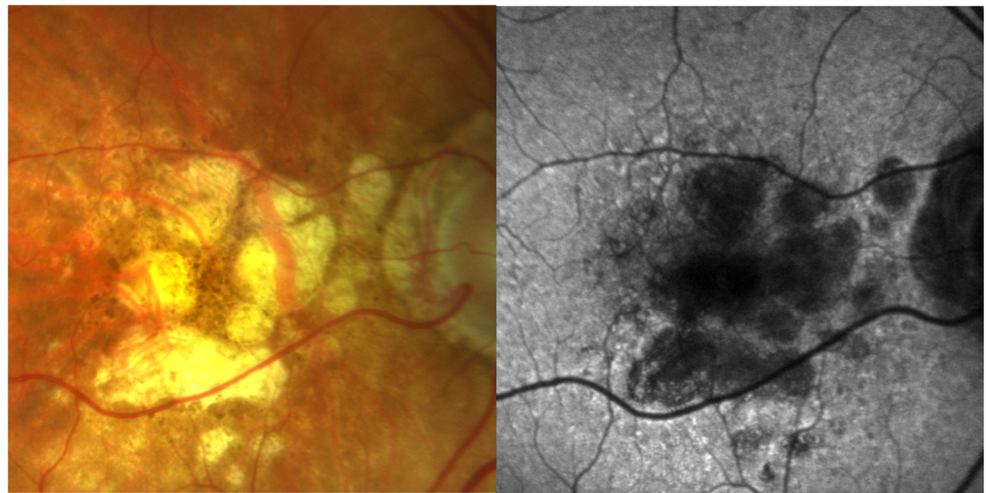
0.81 mm²/year). Rates of enlargement were higher in eyes with more pronounced increases in FAF, such as the banded (median 1.81 mm²/year) or diffuse (median 1.77 mm²/year) patterns. The comparison of progression rates between the "none" or "focal" groups on one hand, and the "banded" or "diffuse" groups on the other revealed a statistically significant difference ($p < 0.0001$) [34]. Although these patterns may reflect heterogeneity on a molecular, cellular, or genetic level, significant risk loci for susceptibility to GA in AMD could not be shown to affect GA progression. [38] The data analyzed by Schmitz-Valckenberg et al. [39] and Bearely et al. [40] on the area of increased FAF around atrophy and its influence on atrophy enlargement support the hypothesis of a pathophysiological role for LF accumulation in RPE cell death. Other prognostic factors for GA progression have also been



Fig. 5 Left eye of a patient with intermediate AMD characterized by large soft confluent drusen and areas of focal hyperpigmentation (a). Reticular pseudodrusen can be seen more clearly in FAF (b) than in CFP (a). In an infrared reflectance (IR) image (c), soft drusen

correspond to increased signal intensity, and reticular pseudodrusen appear as a pattern-like grouping of ill-defined lesions with lower reflectivity. Fluorescein angiography at the late phase reveals pronounced hyperfluorescence due to drusen staining (d)

Fig. 6 Geographic atrophy due to age-related macular degeneration: fundus photography (CFP, left) and fundus autofluorescence (FAF, right). Due to the lack of fluorophore-containing RPE cells, multifocal areas of geographic atrophy are readily identifiable in the FAF image versus the CFP image



described, including knowledge of prior rates of enlargement [41] or enlargement rate of the fellow eye [42, 41], multifocal configuration of GA [7], baseline GA size [41, 34], and diagnosis of the fellow eye [43].

Natural history data and identification of high-risk characteristics are important for the design of interventional clinical trials aimed at reducing the progression of in GA. The FDA recently accepted GA lesion growth—a morphological endpoint—as a main outcome parameter in GA studies, and it is now used in almost all ongoing interventional trials [33].

Foveal sparing

GA patches typically occur initially in the parafoveal retina. With the spread of GA over time, several atrophic areas may coalesce, and new atrophic areas may occur. In advanced stages, GA areas may form a ring encompassing the intact and still-functioning fovea. On clinical examination, the fovea may remain uninvolved in the atrophic process until late in the course of the disease, a phenomenon referred to as “foveal sparing” [44, 45]. Areas of GA are associated with a

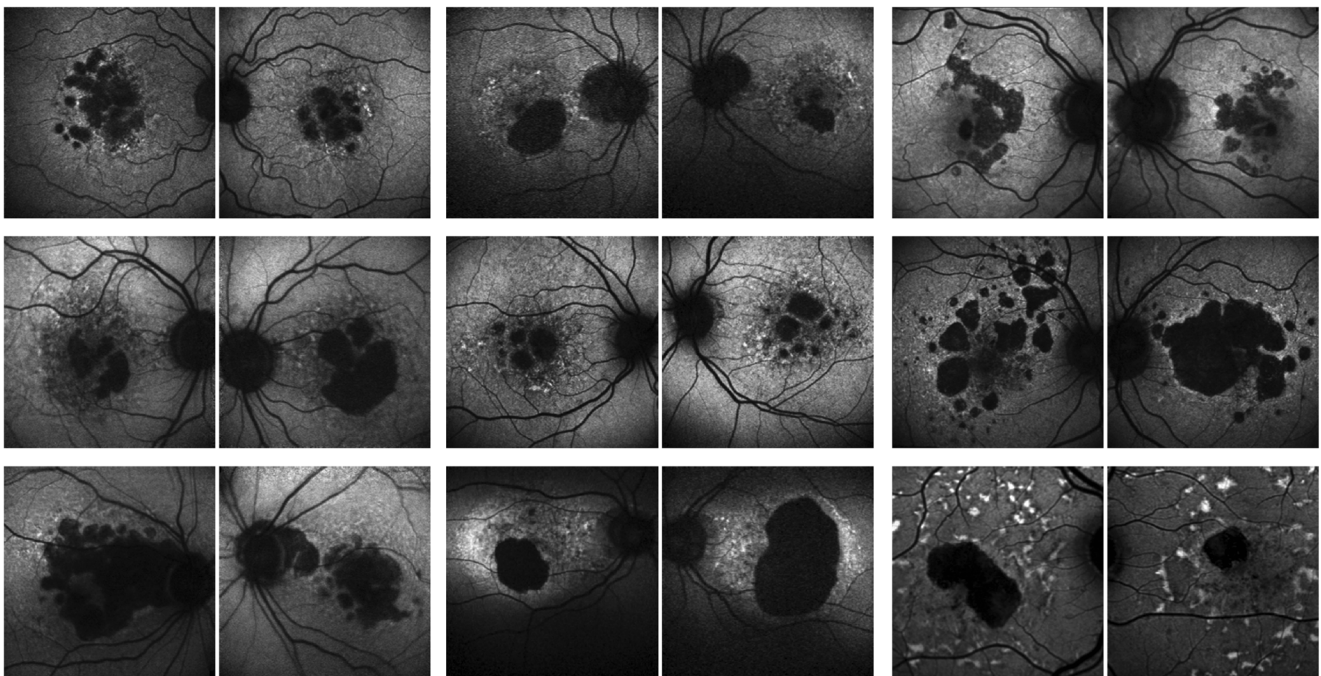
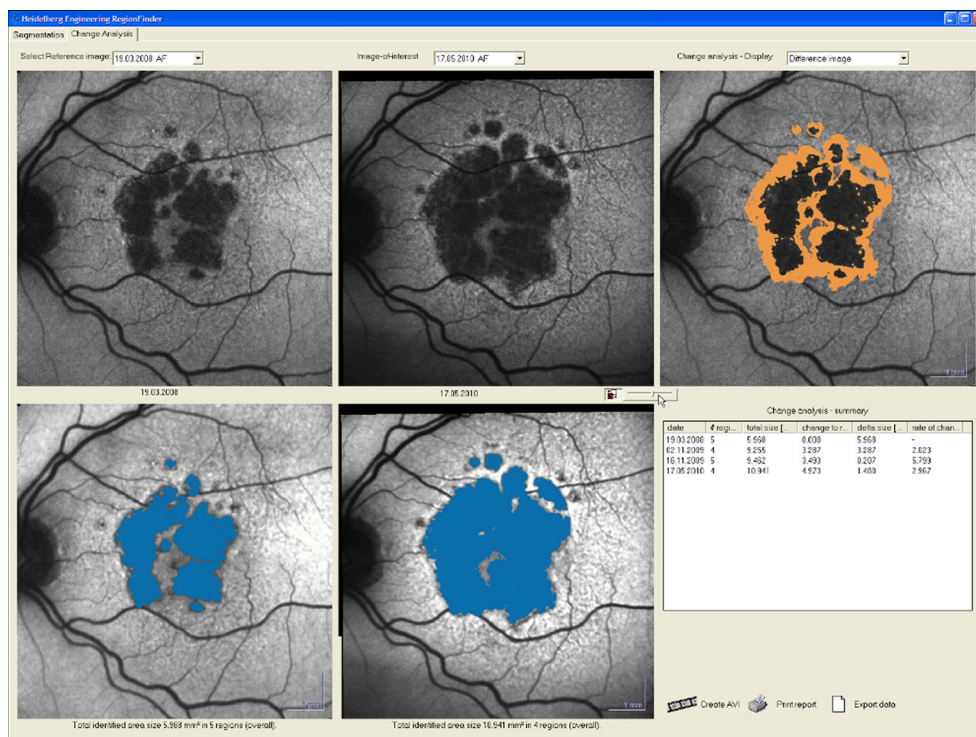


Fig. 7 Fundus autofluorescence (FAF) images of both eyes from various patients with unifocal and multifocal geographic atrophy. Note the high degree of intraindividual symmetry between the eyes and interindividual heterogeneity with regard to the size and topography of geographic atrophy (dark patches reflecting a reduced FAF signal due to the absence

of retinal pigment epithelial cells and their fluorophores). This is also seen in the perilesional abnormal patterns of increased FAF signals surrounding the atrophic patches. Elsevier, as the copyright holder, has kindly granted copyright permission for the use of this figure, which was adapted from Holz et al. [51]

Fig. 8 Semi-automated quantification of geographic atrophy (GA) by means of image analysis software (RegionFinder, Heidelberg Engineering, Heidelberg, Germany). Areas of atrophy can be quantified in a precise, reproducible, and time-effective way. In this example, the difference image on the right shows the enlargement (orange) of geographic atrophy between baseline (left) and follow-up visit (middle). Adapted from Fleckenstein et al. [52]



corresponding absolute scotoma. Thus, the “foveal sparing” pattern of disease evolution corresponds with progressive visual impairment, which is initially characterized by reading difficulties due to parafoveal scotomata, while the central visual acuity is preserved [46, 44, 26, 47, 6]. When the fovea finally becomes involved, a dramatic loss in visual acuity

occurs. After involvement of the central macula, relatively little benefit can be expected from any future therapeutic intervention attempting to slow or halt the natural course of the disease [48, 49]. Although atrophic patches exhibit an even lower FAF intensity than the central macula, foveal involvement can be challenging to identify (Fig. 10) [31,

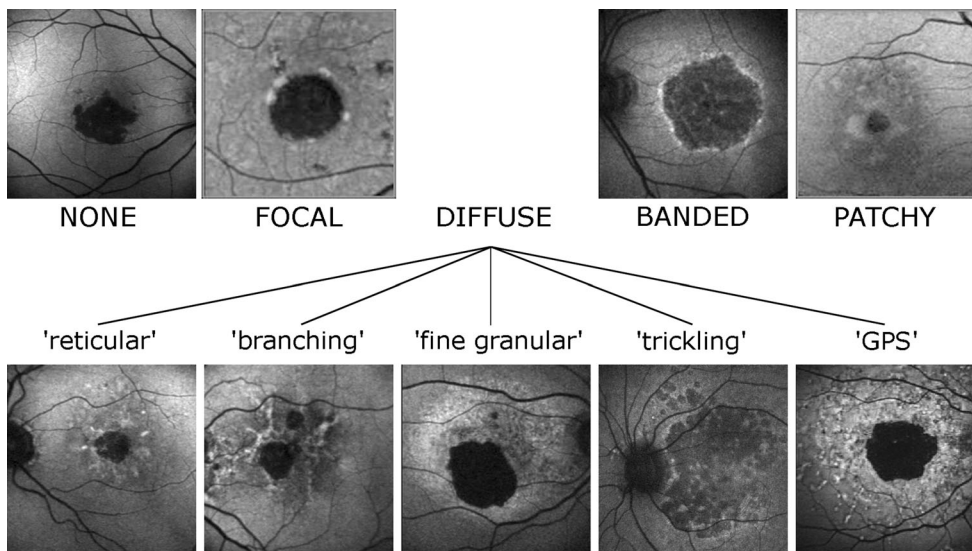


Fig. 9 Dominant phenotypic patterns of abnormal FAF in the junctional zone of GA based on confocal scanning laser ophthalmoscopy (cSLO) fundus autofluorescence (FAF) imaging. These patterns have prognostic relevance for disease progression in terms of atrophic enlargement over time. While patterns with little change in FAF intensities surrounding the GA predispose to slow progression, the banded and all diffuse patterns

representing more pronounced increases in FAF are frequently accompanied by high progression rates. The Association for Research in Vision and Ophthalmology (ARVO), as the copyright holder, has kindly granted copyright permission for the use of this figure, which was adapted from Fritsche et al. [28]

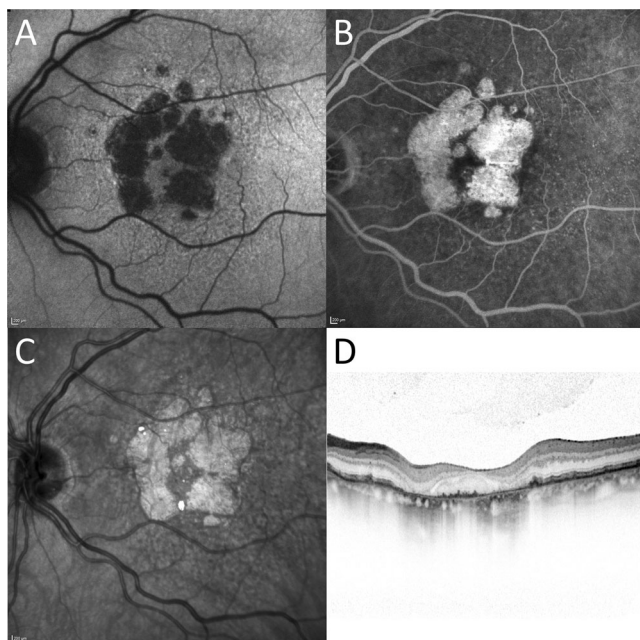


Fig. 10 GA with foveal sparing, shown in different imaging modalities. **a**, in FAF, atrophic areas appear dark due to their lack of lipofuscin. The border towards the intact fovea is essentially indistinct, as lipofuscin fluorescence is largely obscured by overlying foveal pigment. **b**, in fluorescent angiograms, the fluorescein-filled choriocapillaris is visible through the GA area. **c**, in near-infrared images, GA areas appear brighter, and the contrast to the intact retina is generally less pronounced; however, foveal sparing is better visualized than in FAF. **d**, optical coherence tomograms visualize the atrophic pigment epithelium and photoreceptor degeneration

50]. Additional use of near-infrared reflectance (IR) cSLO images has been proven helpful in determining foveal sparing (Fig. 10) [31].

We recently quantified differential spread characteristics centrifugally vs. centripetally in eyes with foveal-sparing GA due to AMD. Peripheral progression and foveal regression were correlated only to a degree, suggesting systematic differences within the group of GA with foveal sparing. Such data will help to design future interventional trials in GA aimed at prolonging foveal survival.

Ophthalmic imaging technology has revolutionized retinal examination. Imaging systems have contributed significantly to our understanding of the pathophysiology, natural history, and treatment of retinal diseases. With the advent of cSLO imaging technology, FAF imaging can be performed with high spatial resolution in a non-invasive and non-time-consuming fashion. Particularly in dry AMD, FAF provides information over and above conventional imaging techniques. It has become the gold standard for the imaging of geographic atrophy due to AMD and for quantification of lesion size, which are now used as primary anatomic outcome parameters for interventional clinical trials in patients with GA. Ongoing developments include quantification of the

fluorophore-derived signal (quantitative autofluorescence), autofluorescence-based molecular imaging, as well as refined structure–function correlations.

Conflict of interest Frank G. Holz is a consultant for Acucela, Alcon, Allergan, Bayer HealthCare, Genentech, Heidelberg Engineering, Novartis, and Roche. He has received research funding from Alcon, Allergan, Bayer, Genentech, Heidelberg Engineering, Novartis, Optos, Roche and Carl Zeiss Meditec.

Steffen Schmitz-Valckenberg is a consultant for Novartis. He has received research funding from Alcon, Allergan, Bayer, Genentech, Heidelberg Engineering, Merz Pharmaceuticals, Novartis, Optos, Roche and Carl Zeiss Meditec.

Monika Fleckenstein is a consultant for Roche/Genentech. She has received research funding from Genentech, Heidelberg Engineering, Novartis, and Optos.

Julia S. Steinberg has no conflict of interest to declare.

Arno Göbel has received research funding from Carl Zeiss Meditec, Heidelberg Engineering, and Optos.

References

- Schmitz-Valckenberg S, Holz FG, Bird AC, Spaide RF (2008) Fundus autofluorescence imaging: review and perspectives. *Retina* 28(3):385–409. doi:10.1097/IAE.0b013e318164a907
- von Rückmann A, Fitzke FW, Bird AC (1995) Distribution of fundus autofluorescence with a scanning laser ophthalmoscope. *Br J Ophthalmol* 79(5):407–412
- Delori FC, Dorey CK, Staurengi G, Arend O, Goger DG, Weiter JJ (1995) In vivo fluorescence of the ocular fundus exhibits retinal pigment epithelium lipofuscin characteristics. *Invest Ophthalmol Vis Sci* 36(3):718–729
- Kellner U, Kellner S, Weinitz S (2010) Fundus autofluorescence (488 NM) and near-infrared autofluorescence (787 NM) visualize different retinal pigment epithelium alterations in patients with age-related macular degeneration. *Retina* 30(1):6–15
- Schatz H, McDonald HR (1989) Atrophic macular degeneration. Rate of spread of geographic atrophy and visual loss. *Ophthalmology* 96(10):1541–1551
- Sunness JS, Rubin GS, Applegate CA, Bressler NM, Marsh MJ, Hawkins BS, Haselwood D (1997) Visual function abnormalities and prognosis in eyes with age-related geographic atrophy of the macula and good visual acuity. *Ophthalmology* 104(10):1677–1691
- Klein R, Meuer SM, Knudtson MD, Klein BE (2008) The epidemiology of progression of pure geographic atrophy: the beaver dam eye study. *Am J Ophthalmol* 146(5):692–699. doi:10.1016/j.ajo.2008.05.050
- Boulton M, Dayhaw-Barker P (2001) The role of the retinal pigment epithelium: topographical variation and ageing changes. *Eye (Lond)* 15(Pt 3):384–389. doi:10.1038/eye.2001.141
- Schmitz-Valckenberg S, Steinberg JS, Fleckenstein M, Visvalingam S, Brinkmann CK, Holz FG (2010) Combined confocal scanning laser ophthalmoscopy and spectral-domain optical coherence tomography imaging of reticular drusen associated with age-related macular degeneration. *Ophthalmology* 117(6):1169–1176. doi:10.1016/j.ophtha.2009.10.044
- Ferris FL 3rd, Wilkinson CP, Bird A, Chakravarthy U, Chew E, Csaky K, Sadda SR (2013) Clinical classification of age-related macular degeneration. *Ophthalmology* 120(4):844–851. doi:10.1016/j.ophtha.2012.10.036
- Mimoun G, Soubrane G, Coscas G (1990) Macular drusen. *J Fr Ophthalmol* 13(10):511–530

12. Bindewald A, Bird AC, Dandekar SS, Dolar-Szczasny J, Dreyhaupt J, Fitzke FW, Einbock W, Holz FG, Jorzik JJ, Keilhauer C, Lois N, Mlynski J, Pauleikhoff D, Staurengli G, Wolf S (2005) Classification of fundus autofluorescence patterns in early age-related macular disease. *Invest Ophthalmol Vis Sci* 46(9):3309–3314. doi:10.1167/iov.04-0430
13. Lois N, Owens SL, Coco R, Hopkins J, Fitzke FW, Bird AC (2002) Fundus autofluorescence in patients with age-related macular degeneration and high risk of visual loss. *Am J Ophthalmol* 133(3):341–349
14. Delori FC, Fleckner MR, Goger DG, Weiter JJ, Dorey CK (2000) Autofluorescence distribution associated with drusen in age-related macular degeneration. *Invest Ophthalmol Vis Sci* 41(2):496–504
15. Landa G, Rosen RB, Pilavas J, Garcia PM (2012) Drusen characteristics revealed by spectral-domain optical coherence tomography and their corresponding fundus autofluorescence appearance in dry age-related macular degeneration. *Ophthalmic Res* 47(2):81–86. doi:10.1159/000324988
16. Pilotto E, Guidolin F, Convento E, Spedicato L, Vujosevic S, Cavarzeran F, Midena E (2013) Fundus autofluorescence and microperimetry in progressing geographic atrophy secondary to age-related macular degeneration. *Br J Ophthalmol* 97(5):622–626. doi:10.1136/bjophthalmol-2012-302633
17. Toy BC, Krishnadev N, Indaram M, Cunningham D, Cukras CA, Chew EY, Wong WT (2013) Drusen regression is associated with local changes in fundus autofluorescence in intermediate age-related macular degeneration. *Am J Ophthalmol* 156(3):532–542 e531. doi:10.1016/j.ajo.2013.04.031
18. Klein R, Davis MD, Magli YL, Segal P, Klein BE, Hubbard L (1991) The Wisconsin age-related maculopathy grading system. *Ophthalmology* 98(7):1128–1134
19. Arnold JJ, Sarks SH, Killingsworth MC, Sarks JP (1995) Reticular pseudodrusen. A risk factor in age-related maculopathy. *Retina* 15(3):183–191
20. Smith RT, Sohrab MA, Busuioic M, Barile G (2009) Reticular macular disease. *Am J Ophthalmol* 148(5):733–743. doi:10.1016/j.ajo.2009.06.028
21. Zweifel SA, Spaide RF, Curcio CA, Malek G, Imamura Y (2010) Reticular pseudodrusen are subretinal drusenoid deposits. *Ophthalmology* 117(2):303–312. doi:10.1016/j.ophtha.2009.07.014
22. Schmitz-Valckenberg S, Alten F, Steinberg JS, Jaffe GJ, Fleckenstein M, Mukesh BN, Hohman TC, Holz FG (2011) Reticular drusen associated with geographic atrophy in age-related macular degeneration. *Invest Ophthalmol Vis Sci* 52(9):5009–5015. doi:10.1167/iov.11-7235
23. Finger RP, Wu Z, Luu CD, Kearney F, Ayton LN, Lucci LM, Hubbard WC, Hageman JL, Hageman GS, Guymer RH (2014) Reticular pseudodrusen: a risk factor for geographic atrophy in fellow eyes of individuals with unilateral choroidal neovascularization. *Ophthalmology*. doi:10.1016/j.ophtha.2013.12.034
24. Pumariega NM, Smith RT, Sohrab MA, Letien V, Souied EH (2011) A prospective study of reticular macular disease. *Ophthalmology* 118(8):1619–1625. doi:10.1016/j.ophtha.2011.01.029
25. Steinberg JS, Auge J, Jaffe GJ, Fleckenstein M, Holz FG, Schmitz-Valckenberg S (2013) Longitudinal analysis of reticular drusen associated with geographic atrophy in age-related macular degeneration. *Invest Ophthalmol Vis Sci* 54(6):4054–4060. doi:10.1167/iov.12-11538
26. Schmitz-Valckenberg S, Bultmann S, Dreyhaupt J, Bindewald A, Holz FG, Rohrschneider K (2004) Fundus autofluorescence and fundus perimetry in the junctional zone of geographic atrophy in patients with age-related macular degeneration. *Invest Ophthalmol Vis Sci* 45(12):4470–4476. doi:10.1167/iov.03-1311
27. Pilotto E, Benetti E, Convento E, Guidolin F, Longhin E, Parozzani R, Midena E (2013) Microperimetry, fundus autofluorescence, and retinal layer changes in progressing geographic atrophy. *Can J Ophthalmol* 48(5):386–393. doi:10.1016/j.cjco.2013.03.022
28. Fritsche LG, Fleckenstein M, Fiebig BS, Schmitz-Valckenberg S, Bindewald-Wittich A, Keilhauer CN, Renner AB, Mackensen F, Mössner A, Pauleikhoff D, Adrion C, Mansmann U, Scholl HP, Holz FG, Weber BH (2012) A subgroup of age-related macular degeneration is associated with mono-allelic sequence variants in the ABCA4 gene. *Invest Ophthalmol Vis Sci* 53(4):2112–2118. doi:10.1167/iov.11-8785
29. Zhou J, Jang YP, Kim SR, Sparrow JR (2006) Complement activation by photooxidation products of A2E, a lipofuscin constituent of the retinal pigment epithelium. *Proc Natl Acad Sci U S A* 103(44):16182–16187. doi:10.1073/pnas.0604255103
30. Bergmann M, Schutt F, Holz FG, Kopitz J (2004) Inhibition of the ATP-driven proton pump in RPE lysosomes by the major lipofuscin fluorophore A2-E may contribute to the pathogenesis of age-related macular degeneration. *FASEB J* 18(3):562–564. doi:10.1096/fj.03-0289fje
31. Schmitz-Valckenberg S, Brinkmann CK, Alten F, Herrmann P, Stratmann NK, Göbel AP, Fleckenstein M, Diller M, Jaffe GJ, Holz FG (2011) Semiautomated image processing method for identification and quantification of geographic atrophy in age-related macular degeneration. *Invest Ophthalmol Vis Sci* 52(10):7640–7646. doi:10.1167/iov.11-7457
32. Lindblad AS, Lloyd PC, Clemons TE, Gensler GR, Ferris FL 3rd, Klein ML, Armstrong JR (2009) Change in area of geographic atrophy in the Age-related Eye disease study: AREDS report number 26. *Arch Ophthalmol* 127(9):1168–1174. doi:10.1001/archophthalmol.2009.198
33. Csaky KG, Richman EA, Ferris FL 3rd (2008) Report from the NEI/FDA ophthalmic clinical trial design and endpoints symposium. *Invest Ophthalmol Vis Sci* 49(2):479–489. doi:10.1167/iov.07-1132
34. Holz FG, Bindewald-Wittich A, Fleckenstein M, Dreyhaupt J, Scholl HP, Schmitz-Valckenberg S (2007) Progression of geographic atrophy and impact of fundus autofluorescence patterns in age-related macular degeneration. *Am J Ophthalmol* 143(3):463–472. doi:10.1016/j.ajo.2006.11.041
35. Mausitz MM, Fonseca S, Chang P, Göbel AP, Fleckenstein M, Jaffe GJ, Holz FG, Schmitz-Valckenberg S (2012) Topography of geographic atrophy in age-related macular degeneration. *Invest Ophthalmol Vis Sci* 53(8):4932–4939. doi:10.1167/iov.12-9711
36. Fleckenstein M, Schmitz-Valckenberg S, Lindner M, Bezatis A, Becker E, Fimmers R, Holz FG (2014) The “diffuse-trickling” fundus autofluorescence phenotype in geographic atrophy. *Invest Ophthalmol Vis Sci*. doi:10.1167/iov.13-13409
37. Fleckenstein M, Charbel Issa P, Helb HM, Schmitz-Valckenberg S, Finger RP, Scholl HP, Loeffler KU, Holz FG (2008) High-resolution spectral domain-OCT imaging in geographic atrophy associated with age-related macular degeneration. *Invest Ophthalmol Vis Sci* 49(9):4137–4144. doi:10.1167/iov.08-1967
38. Scholl HP, Fleckenstein M, Fritsche LG, Schmitz-Valckenberg S, Göbel A, Adrion C, Herold C, Keilhauer CN, Mackensen F, Mössner A, Pauleikhoff D, Weinberger AW, Mansmann U, Holz FG, Becker T, Weber BH (2009) CFH, C3 and ARMS2 are significant risk loci for susceptibility but not for disease progression of geographic atrophy due to AMD. *PLoS ONE* 4(10):e7418. doi:10.1371/journal.pone.0007418
39. Schmitz-Valckenberg S, Bindewald-Wittich A, Dolar-Szczasny J, Dreyhaupt J, Wolf S, Scholl HP, Holz FG (2006) Correlation between the area of increased autofluorescence surrounding geographic atrophy and disease progression in patients with AMD. *Invest Ophthalmol Vis Sci* 47(6):2648–2654. doi:10.1167/iov.05-0892
40. Bearely S, Khanifar AA, Lederer DE, Lee JJ, Ghodasra JH, Stinnett SS, Cousins SW (2011) Use of fundus autofluorescence images to predict geographic atrophy progression. *Retina* 31(1):81–86. doi:10.1097/IAE.0b013e3181e0958b
41. Sunness JS, Margalit E, Srikanth D, Applegate CA, Tian Y, Perry D, Hawkins BS, Bressler NM (2007) The long-term natural history of

- geographic atrophy from age-related macular degeneration: enlargement of atrophy and implications for interventional clinical trials. *Ophthalmology* 114(2):271–277. doi:10.1016/j.ophtha.2006.09.016
42. Fleckenstein M, Adrion C, Schmitz-Valckenberg S, Göbel AP, Bindewald-Wittich A, Scholl HP, Mansmann U, Holz FG (2010) Concordance of disease progression in bilateral geographic atrophy due to AMD. *Invest Ophthalmol Vis Sci* 51(2):637–642. doi:10.1167/iovs.09-3547
43. Fleckenstein M, Schmitz-Valckenberg S, Adrion C, Visvalingam S, Göbel AP, Mössner A, von Strachwitz CN, Mackensen F, Pauleikhoff D, Wolf S, Mansmann U, Holz FG (2011) Progression of age-related geographic atrophy: role of the fellow eye. *Invest Ophthalmol Vis Sci* 52(9):6552–6557. doi:10.1167/iovs.11-7298
44. Sunness JS, Bressler NM, Maguire MG (1995) Scanning laser ophthalmoscopic analysis of the pattern of visual loss in age-related geographic atrophy of the macula. *Am J Ophthalmol* 119(2):143–151
45. Sarks JP, Sarks SH, Killingsworth MC (1988) Evolution of geographic atrophy of the retinal pigment epithelium. *Eye (Lond)* 2(Pt 5):552–577. doi:10.1038/eye.1988.106
46. Sunness JS (1999) The natural history of geographic atrophy, the advanced atrophic form of age-related macular degeneration. *Mol Vis* 5:25
47. Forte R, Querques G, Querques L, Leveziel N, Benhamou N, Souied EH (2013) Multimodal evaluation of foveal sparing in patients with geographic atrophy due to age-related macular degeneration. *Retina* 33(3):482–489. doi:10.1097/IAE.0b013e318276e11e
48. Maguire P, Vine AK (1986) Geographic atrophy of the retinal pigment epithelium. *Am J Ophthalmol* 102(5):621–625
49. Sunness JS, Gonzalez-Baron J, Applegate CA, Bressler NM, Tian Y, Hawkins B, Barron Y, Bergman A (1999) Enlargement of atrophy and visual acuity loss in the geographic atrophy form of age-related macular degeneration. *Ophthalmology* 106(9):1768–1779. doi:10.1016/S0161-6420(99)90340-8
50. Schmitz-Valckenberg S, Fleckenstein M, Helb HM, Charbel Issa P, Scholl HP, Holz FG (2009) In vivo imaging of foveal sparing in geographic atrophy secondary to age-related macular degeneration. *Invest Ophthalmol Vis Sci* 50(8):3915–3921. doi:10.1167/iovs.08-2484
51. Holz FG, Strauss EC, Schmitz-Valckenberg S, van Lookeren CM (2014) Geographic atrophy: clinical features and potential therapeutic approaches. *Ophthalmology* 121(5):1079–1091. doi:10.1016/j.ophtha.2013.11.023
52. Fleckenstein M, Wolf-Schnurrbusch U, Wolf S, von Strachwitz C, Holz FG, Schmitz-Valckenberg S (2010) Imaging diagnostics of geographic atrophy. *Ophthalmologie* 107(11):1007–1015. doi:10.1007/s00347-010-2159-y